# INVESTIGATION OF EXTENDED OVER-WATER RANGES OF LOW-SITED RADAR

*By F. A. Sabransky*

U. S. Navy Electronic Laboratory, San Diego

(Original manuscript received 29 November 1956; revised manuscript received 25 September 1957)

ABSTRACT

An investigation of the extension of radar ranges coincidental with the existence of surface-based super-refractive layers is discussed using data obtained during the operation of a low-sited overwater radar link. Instrument readings were found to agree substantially with results predicted by previously published methods. Individual cases are treated to show the interrelationship with the increase in signal strength and the development of the super-refractive layer as a result of air-mass movement and modification.

## 1. Introduction

A simple method of predicting extended coverage for surface targets by low-sited radar units was developed at the Navy Electronics Laboratory. It was shown that refractive index profiles based upon the micrometeorology of boundary layers could be obtained from standard shipboard weather observations. Techniques for the determination of oceanic duct propagation from statistical meteorological data have been used in making monthly charts of the probability of extended coverage for large areas in the Northwest Pacific and Near East [1; 2; 3; 4; 5].

To test the accuracy of the theoretical prediction a low-sited X-band 3-cm radar link was established using a path over the water with antenna and targets fixed (fig. 1). The purpose was to determine the validity of using extended coverage prediction methods and available meteorological data to predict field strength.

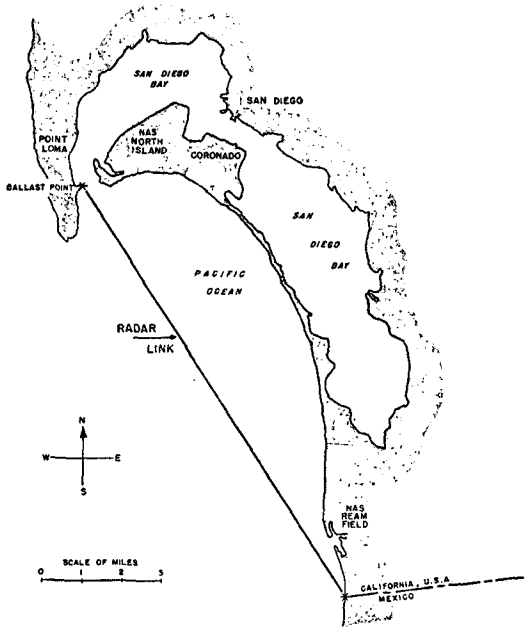


FIG. 1. Site of radar path.

Meteorological data were obtained by stationary measuring apparatus as well as from recording instruments flown through the medium above the path by airplane. The meteorological measurements were examined in conjunction with the radar field strength values to relate the various conditions giving rise to extended or decreased radar coverage.

Preliminary results of the empirical phase of this investigation show agreement with the theory upon which extended coverage prediction is based.

## 2. Radar equipment

In order to accumulate an adequate body of data with which to compare the theoretical propagation predictions, a low-level X-band radar link was established with a 13-mi path over the water. The radar equipment was placed in a small portable building at the edge of the San Diego Bay entrance on Ballast Point, Point Loma. The targets were placed on the lower end of the bight of Coronado Strand, near the Mexican Border. Fig. 1 shows the location of the radar path.

The radar equipment consisted of a range scope (Dumont 256 B A/R) with a transmitter and receiver which had been part of an SU-1 radar. A signal generator (Hewlett-Packard 620A) was used to measure the signal strength by comparison. The antenna was a 24-in parabolic dish located 16.8 ft above mean low-low water and was placed in a fixed position relative to the targets. The gain of the dish was 34 db above isotropic radiation. The peak power output of the transmitter was 40 kw and the frequency of the signal was 9375 Mc (X band).

The targets were three-by-eight foot wooden frames covered with copper screen. One target location was on the beach at an elevation of 16.6 ft above mean low-low water. Two of the three-by-eight foot screens were used at this spot. Care was taken to orient the screens accurately normal to the path of transmission since the beamwidth of a plane reflector is very narrow

at this frequency. The target at mean low-low water was 1.5 statute mi beyond the radio horizon for standard atmospheric conditions.

The other target was situated on a tower near the Mexican Border, 350 yd beyond the low target. This served as a reference target and its elevation was 82.3 ft above the mean low-low water. The location of the reference target placed it about 6 db below the maximum on the height gain curve for average sea level and standard meteorological conditions.

Tide levels to determine the hour by hour height of the radar and targets were obtained from a U. S. Navy tide gauge near the transmitter site. Corrections were made to compensate for the tidal variation over the link.

### 3. Meteorological instrumentation and measurements

Meteorological instrumentation was necessary to study the atmospheric conditions resulting in extended radar coverage. For the purposes of this investigation sampling the atmosphere over the link by standard temperature and humidity elements was satisfactory since profiles of refractive index were not required. Furthermore, the inadequacy of the refractometer in giving *meteorological* information would have been a disadvantage in this study. Air temperatures and wet bulb depressions were also recorded continuously at a fixed height with a thermocouple psychrometer developed by Bellaire and Anderson [6]. The fixed installation was located at an average 25 ft above the surface of the water depending upon the tide level to simulate shipboard measurements. Fig. 2 shows the outside installation located near the transmitter end of the link at the entrance to San Diego Bay. A photoelectric galvanometer amplified the current for continuous recording on an Esterline-Angus recorder.

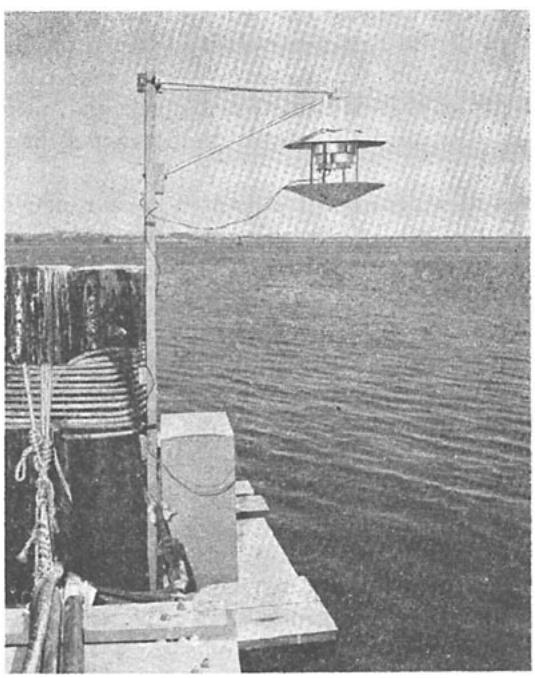

Official United States Naval Photograph

FIG. 2. Tetraskelion containing temperature and wet bulb depression sensing elements.

During periods when meteorological conditions were likely to produce good ducting with subsequent extended radar coverage a thorough investigation of the air mass over the path was undertaken by use of temperature and humidity elements carried by airplane. The temperature and wet bulb sensing elements were Friez ceramic temperature rods in a dc bridge circuit. The element recording wet bulb temperature was wrapped in damp wicking which obtained its moisture from a reservoir that also served as a mounting for the elements. Two microammeters indicated the current change with temperature. By means of a simple conversion table this was read as dry and wet bulb temperature. The temperature measuring unit was inserted in a cylindrical aluminum radiation shield and attached to the wing strut of a low-speed observation plane (U. S. Marine Corps OE-3). Fig. 3 shows this equipment unassembled.

Samples were taken over the link at altitudes ranging from 25 ft up to 2000 ft. Simultaneous sea-surface temperature readings were obtained by boat along the path. When an airplane was not available, soundings were occasionally taken by sling psychrometer at intervals up the windward slope of Point Loma where readings were obtained from the surface to four hundred feet in height. The effects of turbulence restricted this type of sounding to those periods when the wind was almost parallel to the Point. Fortunately, this type of circulation was likely to occur during times of good ducting. Such soundings appeared to be quite reliable when compared with simultaneous soundings taken by aircraft.

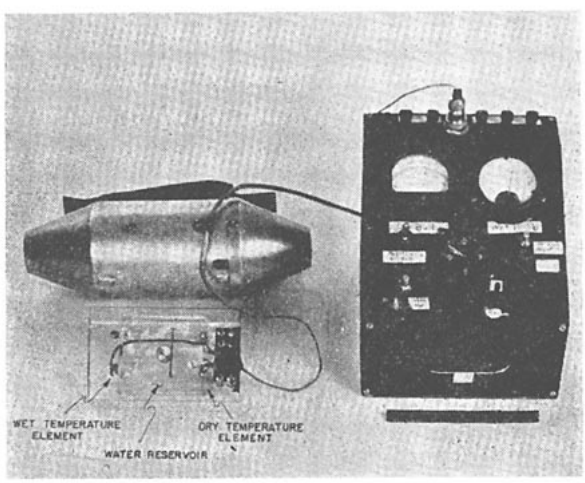


FIG. 3. Temperature and humidity measuring apparatus used in taking airplane soundings over the path.

### 4. Sources of additional meteorological data

Sea-surface temperature readings were furnished by Scripps Institution of Oceanography from measurements taken in the ocean off Scripps pier at La Jolla about five miles north of the link area. It was found that readings here most nearly approximated temperatures along the path taken by small boat. Readings near the radar site were subject to variation as the tide moved in and out of the bay entrance.

Surface wind speed and direction were obtained from continuously recorded measurements taken at the U. S. Naval Air Station, Ream Field, which is located on the coast near the mid-path. The instruments from which this information was taken consisted of a Bendix Aerovane and a wind recorder (Bureau of Aeronautics, NAX 1–4B). These measurements were considered to be representative of wind velocity over the link in most cases.

Further meteorological data were obtained from the morning and evening radiosonde measurements taken by the U. S. Naval Air Station, North Island, which was not far from the path. Wind trajectories were plotted from hourly airways reports issued by civilian and military weather stations throughout Southern California. United States Weather Bureau facsimile maps were continuously received and cover the general meteorological situation.

### 5. Radio-meteorology of the surface duct

The radar propagation prediction method used in this investigation is based upon the existence of a recurrent oceanic surface duct caused by evaporation from the sea surface. In the San Diego area the duct is often associated with a well defined surface-based inversion. The energy from the radar transmitter is guided around the curve of the earth when the surface duct is sufficiently thick and intense to trap the wavelength used by the radar. When the surface super-refractive layer is weakly defined, most of the energy can be regarded as having leaked into the atmosphere so that little reaches targets beyond the horizon.

Oceanic ducts can be the result of evaporation from the sea producing negative humidity gradients over wide oceanic areas. Surface ducts are also formed when dry air from large land masses is carried out over the ocean where evaporation and cooling at the surface again creates a super-refractive layer.

Anderson and Gossard [1; 2] have used the relation

$$\phi - \phi_0 \alpha \int_{z_0}^{h_1} h^{-\beta} dh \qquad (1)$$

to represent the theoretical refractive index profile within the boundary layer where the parameters are defined as:

$h$ height in feet above sea surface at which $\phi$ is measured.
$\beta$ profile index, a function of stability.
$Z_0$ surface roughness parameter.
$\phi$ potential refractive index $= 79/\theta[1000 + (4790/\theta)e_p]$
$\phi_0$ potential refractive index at the surface ($h = 0$)
$\theta$ potential temperature (K)
$e_p$ potential vapor pressure (mb).

When the air above the sea is thermally unstable, *i.e.*, colder than the sea surface, the profile index exceeds unity ($\beta > 1$). When $\beta < 1.0$ the air is stable. An empirical relation between $\beta$ and Richardson's number has been obtained by Deacon [7] for given instrument heights and surface roughness. Corresponding curves for other instrument heights and surface roughness may be calculated from Deacon's data. The surface roughness, $z_0$, is assumed to be 0.6 cm for winds greater than 12 kn and 0.01 cm for winds less than 12 kn.

S. A. Schelkunoff [8] replaces the actual refractive index profile by the two-layer model having the equivalent effect on the vertical distribution of field strength within and above the duct. Schelkunoff's two-layer model assumes the modified refractive index, $M$, to be independent of height above and below an abrupt discontinuity at $H$. One obtains the best fit between the height-gain curve of the two-layer model and that of the actual profile, $M(h)$, as

$$H \int_0^H M(h)dh - H^2 M(H) = (9 \times 10^6/128)\lambda^2 \qquad (2)$$

where $M = (n - 1) \times 10^6 + .048h \cong \phi + 0.04h$ and $\lambda$ is wave length in centimeters. When (1) is substituted into (2) for $M(h)$ the result may be expressed in terms of the parameter.

$$X = \left[ \frac{(3 - \beta)(\beta - 1)}{(0.06)(2 - \beta)} \frac{\Delta\phi}{h^{1-\beta} - Z_0^{1-\beta}} \right]^{3/\beta} \frac{\beta}{3 - \beta}. \qquad (3)$$

Trapping of the first mode occurs when $X$ exceeds the critical value

$$X_c = 3770\lambda^2.$$

### 6. Meteorology of the area

The meteorology of the San Diego region during the six or seven months beginning with October is characterized by frontal systems related to low pressure areas moving across the North Pacific and crossing the Oregon and Washington coast. The lows increase in intensity and frequency during the middle of this period. Prevailing surface winds are variable but generally are westerly to northwesterly and bring in moist, cool, maritime air at lower levels. Occasionally subsidence of the warm dry air aloft causes an elevated inversion which was found to have little effect

on the extension of ranges of the low-level microwave radar over the path used in this experiment. However, no radio data were used in this study for days when the San Diego raob indicated the field could have been strengthened by conditions other than the surface duct.

Due to the proximity of the radar link to the coast an easterly flow in the San Diego region does not result in extended ranges unless the air has had a sufficiently long overwater trajectory for modification to have proceeded for some time. Care must be exercised under these conditions since a misleading value of the parameter $X$ can result. The theoretical model on which the ducting predictions are based assumes modification to have proceeded to a steady state condition. Time since modification began or distance from shore do not appear in the resulting formulae. In fig. 4 the unmodified atmosphere is shown as having a standard $B$ profile[1] over the land at $B_1$, where there is no change in the refractive index with height. Shortly after the arrival of this air over the sea a thin layer next to the surface becomes modified giving rise to a large but shallow change in the profile as indicated at $B_2$. Meteorological observations taken at the height of a low-sited radar would show a large difference in refractive index between the air near the sea surface and the unmodified air which would result in a high value for $X$ but no ducting should actually occur. As the air moving farther out to sea is further modified the layer becomes deeper as shown schematically in fig. 4. The refractive index deficit at the fixed height of measurement will be less at $B_3$ than at $B_2$ and the resulting $X$ not as high. However, the values of $X$ obtained will be more consistent with the trapping effect to be expected.

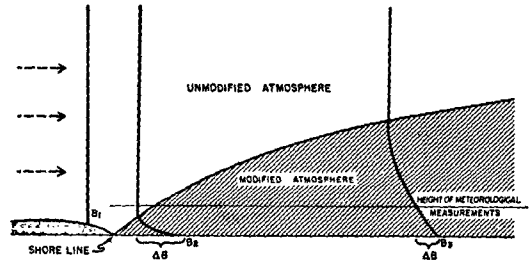


FIG. 4. Sketch showing effects of modification on refractive index B profile.

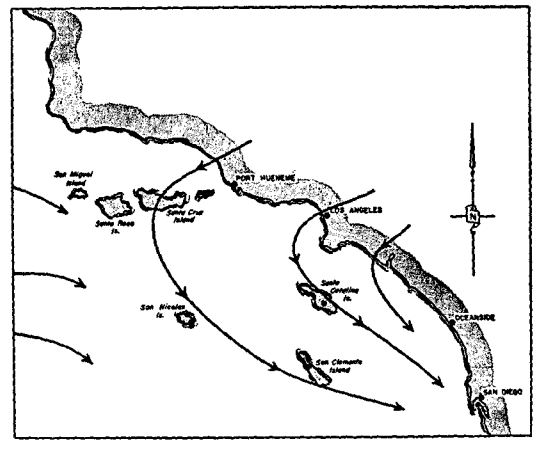


FIG. 5. General pattern of air movement in Southern California resulting in extended coverage for low-lying radar.

[1] The parameter $B = M - 0.036h$ has been used in the figures of this paper because it is more widely familiar to workers in the field of radio propagation than the potential refractive index $\phi$.

In this area, creation of strong surface ducts occurs over the experimental link when warm, dry air moves out over the ocean forty to two hundred miles north of San Diego, and returns in a north-westerly flow over the link. Fig. 5 depicts the general pattern of air movement illustrating this occurrence.

## 7. Comparison of observation with theory

The Ballast Point-Border Field link was not reliably functional until late in the season when regimes giving rise to surface inversions appeared less and less frequently, so that less data were acquired than had been anticipated. However, individual cases show agreement with predictions of extended coverage when air trajectories are taken into account. Fig. 6 gives the results of the operation in terms of a scatter diagram of field strength in db below one milliwatt *vs* $X$. As predicted, when a value of $X$ is obtained which is greater than the critical value indicated by the Schelkunoff formula for the occurrence of trapping, the field strength of the radar signal is increased. At present there are insufficient data to determine whether greater values lead to stronger signals as additional modes are trapped. The majority of the cases of extended coverage occurred on days when the temperature difference between the air and the sea surface indicated thermal stability, *i.e.*, the air temperature was warmer than the sea temperature. The extended coverage noted when unstable conditions existed was generally associated with high wind speeds in agreement with theory.

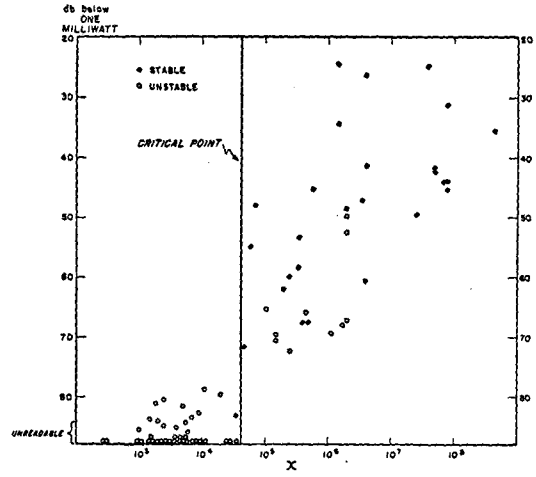


FIG. 6. Scatter diagram showing results of operation.

In addition it can be noted in that portion of fig. 6 above the critical point that the field strengths average lower for the unstable cases than for the stable cases. It is probable that the super-refractive layer during unstable conditions never becomes thick enough to trap more than the first mode.

During the operation, field strengths returned from the higher (reference) target usually exhibited little or no day-to-day variation. There were, however, times when the field strength from this target deviated from its normal behavior. On these occurrences the surface super-refractive layer was exceptionally well defined and the field strength of the return from the low target was high as the result of the complete trapping of the signal. At these times, the field strength of the high target either became erratic, oscillating between weak and strong returns or disappeared completely. Under such conditions an elevated radar installation on a large surface vessel could fail to detect submarine conning towers and snorkels near the sea surface.

## 8. Air mass trajectory and refractive index profiles

The spread of the points in the scatter diagram above the critical level for trapping can be associated with the variation of local air-mass modification. An example of trajectories of the air masses previous to their arrival over the link is shown in fig. 7. The field strengths are also shown. The air movements were traced back to the midnight before the operation of the link. All times given are PST.

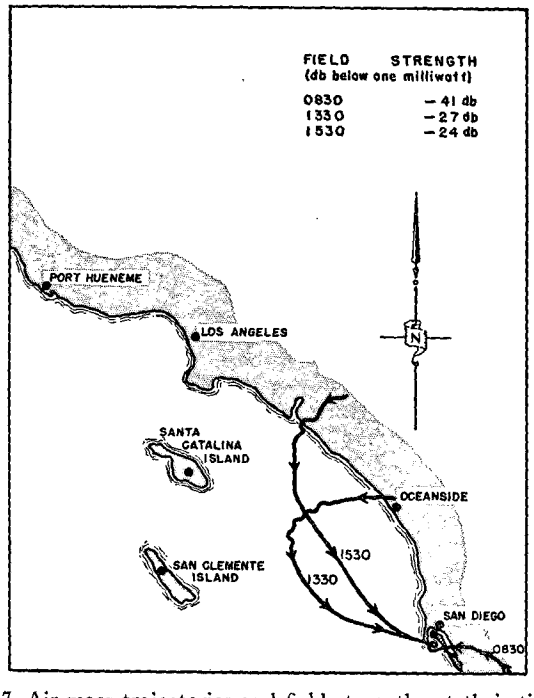


FIG. 7. Air-mass trajectories and field strengths at their time of arrival over the path, 16 March 1956.

Prior to 0830 a gentle easterly breeze had carried dry land air out over the link where it was becalmed. By 0830 this air had been over the area for several hours. Much evaporation and cooling took place next to the water surface. The field strength of the radar at 0830 was 41 db below one milliwatt. While the super-refractive layer was developed enough to result in extended range it was shallow and gave rise to an erroneously high $X$ value of $8 \times 10^7$ (see $b_2$ of fig. 4). In comparison, the air which arrived over the link at 1330 and 1530, respectively, had been swept out to sea north of San Diego and returned to the San Diego area in a north-westerly flow. The longer over-water trajectory led to nearly complete modification as shown by the $B$ profile, fig. 8. Since the super-refractive layer for these two trajectories was well developed the $X$ value of $2 \times 10^6$ reflected the true situation (see $b_3$ of fig. 4).

Fig. 9 shows average modified refractive index profiles obtained from airplane soundings taken over the radar path. The average radar field strength during the time the observations were taken in db below one milliwatt is indicated for each profile. Fig. 9(a) is of particular interest. The $B$ profile came from measurements taken over the link just as the easterly flow from the land was changing to westerly. The thinness of the super-refractive layer is typical of this type of situation. There was much oscillation of the signal, and field strengths varied from between 57 and 77 db

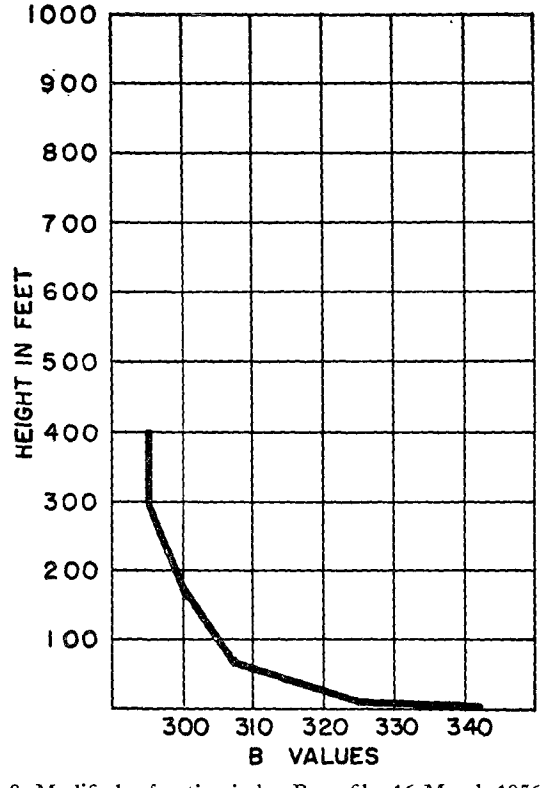


FIG. 8. Modified refractive index B profile, 16 March 1956 from sounding made up the side of Point Loma, 1520 hr.

below one milliwatt. As the westerly wind gained force, bringing with it the air which earlier in the day had moved out from the land to the north of San Diego and which therefore had a long over water trajectory, the field strength increased to 34 db below one milliwatt. Unfortunately, data for constructing the trajectories for the case were not available.

Fig. 9(b) is the $B$ profile for a period of operation when the signal strength was very strong and steady and the super-refractive layer was better developed.

Fig. 9(c) depicts an elevated inversion. There was no increase of the range, and returns from the low target were not received during this regime.

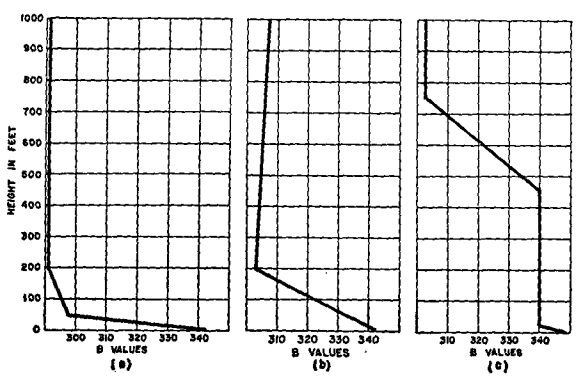


FIG. 9. Modified refractive index profiles developed from airplane soundings with average signal strength for the same period. (a) 1005–1030, 14 May 1956—66 db below one milliwatt, (b) 1425–1445, 15 May 1956—34 db below one milliwatt, (c) 0950–1005, 27 Mar. 1956—Not readable.

## 9. Conclusions

a. Controlled experiments indicate that meteorological data taken by submarines can be used to determine whether extended coverage of surface-to-surface radar can be expected.

b. There are indications that surface ducting may result in loss of coverage of targets very near the surface by radars sited at heights commonly employed on capital ships.

## REFERENCES

1. Anderson, L. J., and E. E. Gossard, 1953: The oceanic duct and its effect on microwave propagation. *Nature*, **172**, 298–300.
2. ——, 1953: The effect of the oceanic duct on microwave propagation. *Trans. Amer. Geophys. Union*, **34**, 695–700.
3. ——, 1955: Prediction of oceanic duct propagation from climatological data. *IRE Trans. Antennas and Propagation*, **AP-3**, 163–167.
4. Radio Meteorology Section, Research Division, 1952: *Far East radio-radar propagation conditions for fleet units.* USN Electronics Lab. Rpt. No. 319.
5. Gossard, E. E., and L. J. Anderson, 1956: *Near East and South East Asia radio-radar propagation conditions for fleet units.* USN Electronics Lab. Rpt. No. 683.
6. Bellaire, F. R., and L. J. Anderson, 1951: Thermocouple psychrometer for field measurements. *Bull. Amer. meteor. Soc.*, **32**, 217–220.
7. Deacon, E. L., 1949: Vertical diffusion in the lowest layers of the atmosphere. *Quart. J. r. meteor. Soc.*, **75**, 89–103.
8. Schelkunoff, S. A., 1944: Microwave transmission in nonhomogeneous atmosphere. *Bell tele. Lab.*, Rpt. MM-44-110-53.